NeuroImage: Clinical 17 (2018) 109–114

Contents lists available at ScienceDirect

NeuroImage: Clinical

journal homepage: www.elsevier.com/locate/ynicl

Integrity of the corpus callosum in patients with periventricular nodular heterotopia related epilepsy by FLNA mutation

Wenyu Liu[a], Dongmei An[a], Running Niu[b], Qiyong Gong[b,*], Dong Zhou[a,**]

[a] Department of Neurology, West China Hospital, Sichuan University, No. 37 GuoXue Alley, Chengdu 610041, China
[b] Department of Radiology, Huaxi MR Research Center (HMRRC), West China Hospital, Sichuan University, No. 37 GuoXue Alley, Chengdu 610041, China

ARTICLE INFO

Keywords:
Corpus callosum
Diffusion abnormality
Epilepsy
FLNA
Periventricular nodular heterotopias

ABSTRACT

Objective: To investigate the quantitative diffusion properties of the corpus callosum (CC) in a large group of patients with periventricular nodular heterotopia (PNH) related epilepsy and to further investigate the effect of *Filamin A* (*FLNA*) mutation on these properties.

Methods: Patients with PNH (n = 34), subdivided into *FLNA*-mutated (n = 11) and *FLNA*-nonmutated patients (n = 23) and healthy controls (n = 34), underwent 3.0 T structural MRI and diffusion imaging scan (64 direction). Fractional anisotropy (FA) and mean diffusivity (MD) were measured in the three major subdivisions of the CC (genu, body and splenium). Correlations between DTI metric changes and clinical parameters were also evaluated. Furthermore, the effect of *FLNA* mutation on structural integrity of the corpus callosum was examined.

Results: Patients with PNH and epilepsy had significant reductions in FA for the genu and splenium of the CC, accompanied by increases in MD for the splenium, as compared to healthy controls. There were no correlations between clinical parameters of epilepsy and MD. The FA value in the splenium negatively correlated with epilepsy duration. Interestingly, *FLNA*-mutated patients showed significantly decreased FA for all three major subdivisions of the CC, and increased MD for the genu and splenium, as compared to HCs and *FLNA*-nonmutated patients.

Conclusions: These findings support the conclusion that patients with epilepsy secondary to PNH present widespread microstructural changes found in the corpus callosum that extend beyond the macroscopic MRI-visible lesions. This study also indicates that *FLNA* may affect white matter integrity in this disorder.

1. Introduction

Malformations of cortical development (MCDs) include a diverse range of disorders that result from defects in the complex process of brain cortical genesis, and are common causes of neurodevelopmental delay and epilepsy (Guerrini and Dobyns, 2014; Leventer et al., 1999). Periventricular nodular heterotopia (PNH) is a commonly encountered epileptic cortical malformation, caused by failure of neurons to migrate away from the embryonic ventricular zone towards the cerebral cortex (Battaglia et al., 2006). Bilateral, symmetrical PNH nodules, particularly in female patients, commonly have a genetic basis related to mutations in *Filamin A* (*FLNA*) gene (Sheen et al., 2001). *FLNA* is a causative gene of PNH and heterozygous mutations cause a wide range of clinical symptoms (Parrini et al., 2006). Asymptomatic PNH may be detected incidentally during brain Magnetic Resonance Imaging (MRI) in cases with no other manifestations (Lange et al., 2015).

Several structural and functional MRI studies have demonstrated that discrete cortical regions are involved in the epileptic network underlying PNH (Christodoulou et al., 2012), and that changes in white matter (WM) integrity are present (Chang et al., 2007). Specifically, several studies have reported morphometric abnormalities in the corpus callosum (CC) (Pardoe et al., 2015; Pisano et al., 2012), and significant diffusion tensor imaging (DTI) metric alterations in the CC (Andrade et al., 2014), as well as other perinodular regions (Filippi et al., 2013) in this disease. Together, these findings confirm the presence of microstructural abnormalities in PNH and provide preliminary support for a diffusion-based endophenotype of this disorder (Kini et al., 2016). However, the diffusion abnormality of the CC in patients with PNH and epilepsy particular has not yet been thoroughly researched. Furthermore, whether the observed CC alterations are related to clinical features, such as epilepsy duration, or differ with respect to *FLNA* mutation, remains an open question.

* Correspondence to: Q. Gong, Department of Radiology, Huaxi MR Research Center (HMRRC), West China Hospital, Sichuan University, Chengdu 610041, China.
** Correspondence to: D. Zhou, Department of Neurology, West China Hospital, Sichuan University, No. 37 GuoXue Alley, Chengdu 610041, China.
E-mail addresses: qiyonggong@hmrrc.org.cn (Q. Gong), zhoudong66@yahoo.de, zd139818@googlemail.com (D. Zhou).

http://dx.doi.org/10.1016/j.nicl.2017.10.002
Received 23 May 2017; Received in revised form 24 September 2017; Accepted 2 October 2017
Available online 13 October 2017

Indeed, CC is the largest fiber bundle in the brain, representing the most important pathway for the inter-hemispheric propagation of epileptic activity (Witelson, 1989). Additionally, its midline position makes it particularly suitable to evaluate in PNH patients, regardless of the heterogeneous nodule locations. Moreover, CC abnormalities have also been reported in other epileptic syndromes (Caligiuri et al., 2016; Thivard et al., 2005).

The aim of this study is to assess microstructural abnormalities in the major segments of the normal-appearing CC in patients with PNH compared to healthy controls (HCs), using DTI measures, and to further investigate the effect of *FLNA* mutation on the integrity of the CC. Correlations between diffusion and clinical parameters were also evaluated. To this end, we recruited PNH patients, who were further subdivided into those carrying a *FLNA* mutation and those without *FLNA* mutations, as well as age- and sex-matched HCs.

2. Methods

2.1. Subject criteria

Patients were recruited from our epilepsy center of West China Hospital, Chengdu, Sichuan province in China. Patients with PNH-related epilepsy were enrolled in this study if their structural MRI showed at least one visible nodule of gray matter signal intensity lining the lateral ventricular walls. The exclusion criteria included the following: (1) additional malformations (e.g. white matter lesions or gross morphometric abnormalities in the CC such as agenesis or dysgenesis); (2) prior brain surgery; (3) MRI incompatibility; (4) history of alcohol/drug abuse, neurological or psychiatric diseases; or (5) pregnant women. There were no criteria regarding age. Patients' demographic and clinical information were collected in detail and underwent routine MRI, electroencephalography (EEG) or long-term video-EEG monitoring. The following clinical features were measured: age at scan, age at seizure onset; epilepsy duration; family history of PNH; family history of epilepsy; history of infantile convulsion; seizure type; seizure frequency; time since last seizure; treatment time and response to antiepileptic drugs (AEDs).

Initially, forty-four patients with a previous diagnosis of PNH with epilepsy were prospectively recruited in this study. Six patients were excluded due to white matter dysplasia; three patients could not tolerate the long imaging time, and one patient had surgery. Ultimately, thirty-four subjects were included. This study was approved by local ethical committee of West China Hospital of Sichuan University; written informed consents were obtained from all subjects or their caregivers.

A comparison group was selected by recruiting the same number of age- and sex-matched right-handed healthy controls (HCs) from the same regional population. Exclusion criteria for healthy comparison group were: (1) any chronic medical disorder, or (2) any convulsive episodes or a family history of epilepsy. Diagnostic quality MR images were taken by two experienced neuroradiologists.

2.2. Gene analysis

Genomic DNA was prepared from patients' peripheral blood. The 47 *FLNA* coding exons (exon 2 to exon 48) and their intron–exon boundaries (Genbank, NC_000023.11) were amplified, with informed consent. The entire *FLNA* coding sequence and flanking splice sites (reference sequence XM_011531131.1) were amplified by PCR. PCR products were sequenced on an ABI 3730 XL automatic sequencer and were analyzed with Seqscanner Software 2 (Applied Biosystems, Foster City, Calif., USA) for potential sequence variations by direct sequencing of PCR products using an ABI Prism Big-Dye Terminator Cycle Sequencing Kit version 3.1 and ABI 3730 XL Avant sequencer (Applied Biosystems, Foster City, Calif., USA).

2.3. Data acquisition

MR scanning was performed on Siemens Trio Tim (3 T) imaging system (Siemens Medical Solutions, Erlangen, Germany). The diffusion-weighted data were obtained using a gradient-echo echo-planar imaging sequence with the following parameters: 64 diffusion directions in the axial plane; TR = 6800 ms; TE = 91 ms; FOV = 240 × 240 mm^2; matrix size = 256 × 256; voxel size = 1.9 × 1.9 × 3.0 mm^3; slice thickness = 3 mm, no slice gap. Additionally, high-resolution three-dimensional T1-weighted structural images were acquired in axial orientation (TR = 1900 ms, TE = 2.26 ms, FOV = 256 × 256 mm^2, matrix = 512 × 512; voxel size = 1 × 1 × 1 mm^3, slice thickness = 1 mm, flip angle = 90°, number of slices = 176). Foam padding was used to minimize head motion and earplugs were used to reduce noise. During data acquisition, subjects were instructed to relax with their eyes closed, and to keep their heads still.

2.4. Data processing

First, the DICOM files of each DWI acquisition were converted into a single multivolume NIFTI file. Eddy current, leading to image distortion, was corrected for each image in FSL (http://www.fmrib.ox.ac.uk/fsl/). The resulting images were co-registered to B0 image using affine transformations to minimize slight head movements. Linear least-squares fitting method was performed to estimate the diffusion tensor models on each voxel using Diffusion Toolkit (Version 0.6.3, Boston, MA). We then executed whole-brain fiber tracking in native diffusion space using the Fiber Assignment by continuous Tracking (FACT) algorithm, which was included in the Diffusion Toolkit (Liao et al., 2011). The cut-off rules of the adopted algorithm were: (1) fractional anisotropy (FA) larger than 1.0, or (2) the angle between the current and the previous path segment exceeded 35 degree (Long et al., 2017). Finally, we co-registered the regions of interest (ROIs) of three major subdivisions of the CC (genu, body and splenium) mentioned above to native diffusion space. Values for FA and MD were then extracted from each ROI for each subject.

To calculate heterotopia volumes, firstly, each nodule or inseparable cluster of nodular tissue was identified and manually outlined within axial slices on T1-weighted images. In this case, we created a heterotopia mask including all nodular tissues for each patient. We counted the number of voxels within the mask of given patients with PNH. Consequently, we have obtained the heterotopia volumes using the numbers of voxels multiply by 1 mm^3.

2.5. Effect of FLNA mutation on diffusion abnormality of the CC

To investigate the effect of *FLNA* mutation on white matter integrity, we used a one-way analysis of covariance (ANCOVA) to characterize the difference of CC integrity in each segments among the three groups (HCs, *FLNA*-mutated patients, and *FLNA*-nonmutated patients).

2.6. Statistical analysis

Statistical analysis was performed using SPSS 20 (IBM, Armonk, New York, USA). An unpaired Student's *t*-test was conducted to determine the differences in the mean FA and MD between the PNH group and control group (InStat 3.10, GraphPad Prism Software, Inc., San Diego, CA). One-way analysis of covariance (ANCOVA) was used to characterize the differences in the CC among the three groups (HCs, *FLNA*-mutated patients, and *FLNA*-nonmutated patients). Further analysis of covariance (ANCOVA) was performed. A p-value < 0.05 (Bonferroni corrected) was considered significant. Effect size was computed to reveal group difference.

3. Results

3.1. Demographic and clinical characteristics

Thirty-four right-handed subjects (22 females, 12 males) with PNH (age at scan [mean ± standard deviation (SD)]: 27.1 ± 10.1 years), were enrolled in the study. The mean duration of seizure was 7.3 years (range: 1–33 years). No patients had cognitive impairment. All patients were treated with antiepileptic drugs (AEDs; 21 on monotherapy and 13 on polytherapy). No patients were drug naïve before MRI scanning. Most patients (29/34, 85.3%) had a history of focal epilepsy (complex partial seizure), and the remaining five patients had primary generalized tonic-clonic seizure. Eight patients were seizure free and five patients had daily to monthly seizures. Eleven patients had *FLNA* mutations.

Thirty-four HCs (23 females; age [mean ± SD]: 27.1 ± 9.9 years, education years [mean ± SD]: 11.5 ± 3.3 years) with no history of neurological disorders, psychiatric illnesses, or abnormalities on MRI examinations were included. The age, sex and education years of the comparison group were not significantly different from the groups of *FLNA*-mutated or *FLNA*-nonmutated patients ($p > 0.05$).

Additionally, the age at scan, age at seizure onset, epilepsy duration, time since last seizure and heterotopia volume did not differ significantly between *FLNA*-mutated and *FLNA*-nonmutated PNH patients (Table 1). Specifically, Student's *t*-test showed the heterotopia volume between two groups was not significantly different (mean volume ± SD: 2827 ± 805.2 mm^3 vs. 1901 ± 1495 mm^3, $p = 0.064$).

3.2. Tractography

Whole brain fiber tracts and tracts passing through the three segments of the CC were detected and visualized using tractography software (Fig. 1). Tractography analysis was not performed for the entire patient group in the current study. Instead, we performed ROI-based analysis due to our interest in the CC itself.

3.3. ROI-based analysis

ROI-based analysis of the CC segments indicated that PNH patients had significant reductions in MD for the splenium of the CC, decreased by 0.000124 ($p = 0.009$, Cohen's $d = 0.65$), accompanied by increases in FA for the genu, increased by 0.0371 ($p = 0.016$, Cohen's $d = 0.59$), and splenium of the CC, increased by 0.0502 ($p = 0.008$, Cohen's $d = 0.67$), as compared to healthy controls. In contrast, there was no significant difference for MD or FA in the body of the CC between the PNH patient group and the HCs (Fig. 2).

There were no correlations between clinical parameters (age, epilepsy duration or time since last seizure) and MD. Only FA value in the splenium segment negatively correlated with disease duration ($r = -0.42$, Bonferroni corrected $p < 0.05$) (Fig. 3).

3.4. Effect of FLNA mutation on CC diffusion abnormality

One-way ANOVA and multiple comparison analysis revealed that *FLNA*-mutated patients showed significant decreased FA in all segments of the CC, and significantly increased MD in the genu and splenium segments of the CC, as compared to HCs and *FLNA*-nonmutated patients. And furthermore, *FLNA*-mutated group patients showed increased MD in the body of the CC compared to the HCs. However, we did not observe any difference for both FA and MD values in all segments in *FLNA*-nonmutated PNH group patients relative to HCs (Fig. 4).

Further analysis of covariance (ANCOVA) was performed and heterotopias volume was treated as a covariate. After adjustment for the factor of heterotopia volume, FA was found to be significantly different between *FLNA*-mutated and *FLNA*-nonmutated groups in all three segments ($p = 0.001$, $p = 0.004$, $p = 0.023$, respectively for genu, body and splenium segments). For the MD, there was only significant difference in the genu and splenium ($p = 0.005$, $p = 0.024$, respectively) between the two groups, but no difference was detected in the body segment ($p = 0.679$).

4. Discussion

In this study, we found that certain segments of the corpus callosum demonstrate decreased FA and increased MD in PNH patients compared to healthy controls, and the correlation between FA in the splenium and epilepsy duration. Furthermore, the differences between *FLNA*-mutated and *FLNA*-nonmutated cases are also evident, suggesting that PNH is associated with altered white matter integrity, and that *FLNA* mutations specifically may influence white matter microstructure. Our results concur with and build on the results of a previous structural study (Andrade et al., 2014), which reported that various subgroups of patients with malformations of cortical development (MCDs), including heterotopia, have diffusion deformations in different parts of the CC.

Our group focused on studying patients with PNH with or without epilepsy (Liu et al., 2017). This disorder characterized by misplaced gray matter nodules (Shafi et al., 2015), is caused by neurons that fail to migrate properly during fetal brain development, which can be associated with mutations in the *FLNA* gene (Parrini et al., 2015). Patients typically present with seizures in adolescence, but they generally have

Table 1
Demographic information of FLNA mutated and FLNA nonmutated patients with PNH, and HCs.

Characteristics	FLNA-mutated patients (n = 11)	FLNA-nonmutated patients (n = 23)	HCs (n = 34)	*p* value
Age (years)	26.4 ± 11.8	27.5 ± 9.5	27.1 ± 9.9	0.956[a]
Sex (male/female)	2/9	9/14	11/23	0.474[b]
Education (years)	9.1 ± 3.7	9.5 ± 3.9	11.5 ± 3.3	0.085[a]
Age at onset (years)	19.6 ± 8.3	19.9 ± 9.1	–	0.933[c]
Epilepsy duration (years)	6.7 ± 8.6	7.6 ± 7.2	–	0.769[c]
Last seizure (months)	8.0 ± 7.9	7.7 ± 7.3	–	0.925[c]
Family history (±)	1/10	0/23	–	0.142[b]
Aura (±)	3/8	7/16	–	0.849[b]
Seizure type (focal/generalized)	9/2	20/3	–	0.692[b]
Previously treated/naïve	11/0	23/0	–	NA
Medication (monotherapy/polytherapy)	7/4	14/9	–	0.876[b]
Treatment timed (years)	5.1 ± 5.3	5.4 ± 2.6	–	0.879[c]
Seizure frequency (> monthly/yearly)	3/8	10/13	–	0.363[b]

Values are mean ± SD.
[a] One-way analysis of variance.
[b] Chi-square test.
[c] Two-tailed two-sample *t*-test.

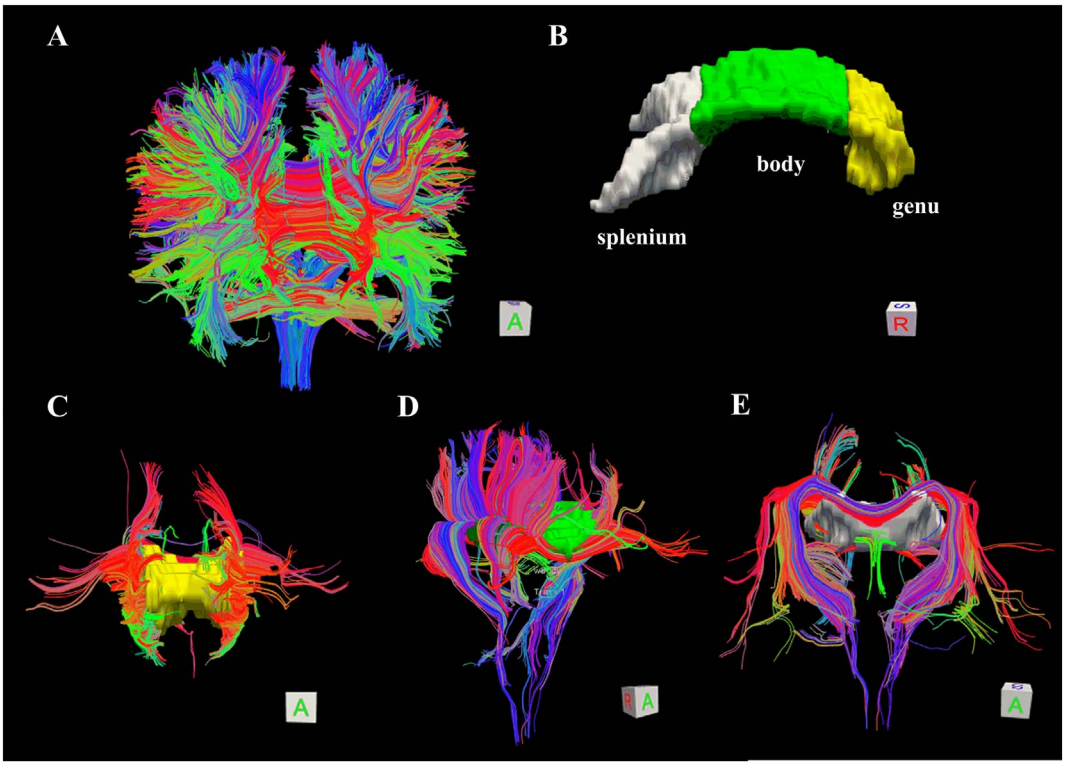

Fig. 1. Image processing with Trackvis in one subject. (A) Whole-brain tractography was obtained from all pixels in the image. (B) The genu, body and splenium subdivisions of the CC were illustrated in yellow, green, and white, respectively. The tracts from the genu (C), body (D) and splenium (E) of the CC were also illustrated. A: anterior view, S: superior view, R: right lateral view.

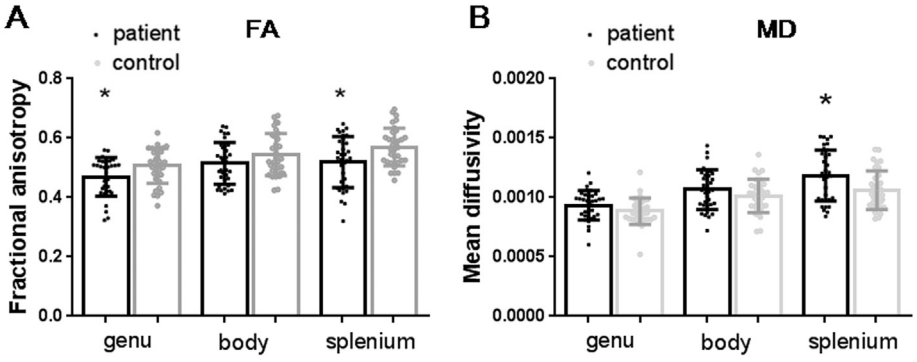

Fig. 2. Comparison of DTI metrics between PNH patients and HCs. The mean values and standard deviation (SD) for FA (A), MD (B), in the genu, body and splenium of the CC in controls (n = 34, gray bars) and PNH patients (n = 32, black bars) were presented. Data originated from the ROI-based analyses; * represents statistically significant differences at Bonferroni corrected $p < 0.05$.

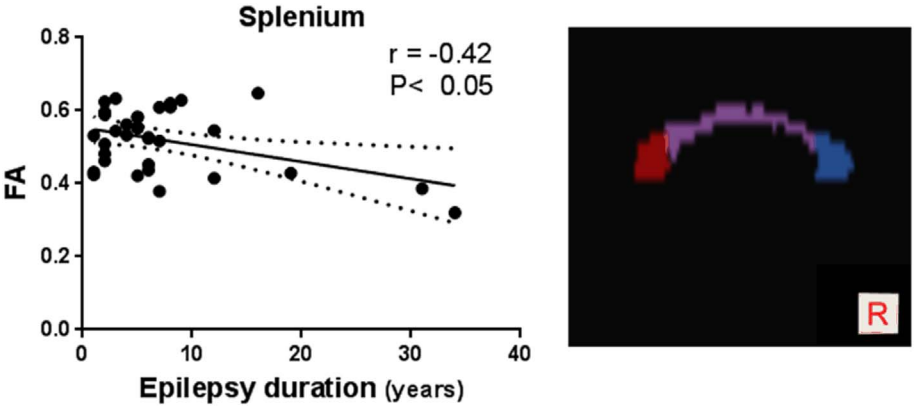

Fig. 3. Correlation between FA value and epilepsy duration in patients with PNH-related epilepsy. FA for the splenium (shown as red color on the right side picture) was negatively correlated with epilepsy duration ($p < 0.05$, Bonferroni corrected). The solid line and dashed lines represent the best-fit line and 95% confidence interval of Pearson correlation. R: right lateral view.

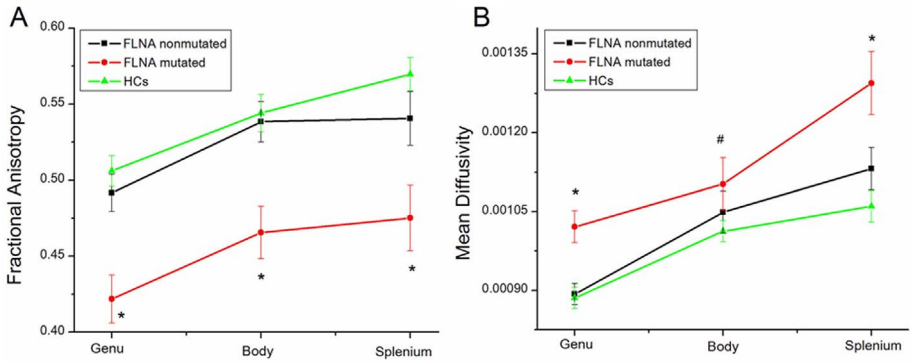

Fig. 4. Comparison of DTI metrics among three subgroups. Mean values and SD for FA (A) and MD (B) derived from the ROI-based analyses were showed, in controls (n = 34, green lines with triangles) and PNH subgroups: *FLNA*-nonmutated group (n = 23, black lines with squares), *FLNA*-mutated group (n = 11, red lines with circles). * represents statistically significant differences at Bonferroni corrected $p < 0.05$, compared to the *FLNA*-nonmutated group and HCs. # represents statistically significant differences at Bonferroni corrected $p < 0.05$, compared to the HCs.

no neurological disabilities, despite this remarkable structural aberration (Battaglia et al., 2006). Previous functional MRI and DTI studies demonstrated that interactions between nodules and cortex may play a major role in the epileptogenesis of PNH (Christodoulou et al., 2012), and found diffusion abnormalities in the perinodular white matter (Filippi et al., 2013) and the CC (Andrade et al., 2014). Overall, the focal perinodular white matter defects in this disorder may serve as the structural basis of developmental dyslexia (Chang et al., 2007). And our study demonstrated that *FLNA* mutations specifically may also influence white matter microstructure of the CC.

Indeed, damage of the CC in mesial temporal lobe epilepsy (mTLE) (Caligiuri et al., 2016), idiopathic generalized epilepsy (IGE) (Ji et al., 2014; Liu et al., 2011) or MCDs including PNH (Eriksson et al., 2001) has been widely reported. The most consistent findings were reduced anisotropy and increased diffusivity in areas of normal-appearing white matter beyond the visible lesions. The CC is a critical pathway for interhemispheric connectivity in the brain (Concha et al., 2007) and participates in brain networks as a central component (Huang et al., 2005). Temporal commissural fibers cross the splenium; prefrontal fibers project to or from the genu and the body contains fibers related to motor cortical areas (Hofer and Frahm, 2006). Moreover, corpus callosotomy can be an effective treatment for some patients with medically intractable epilepsy (Concha et al., 2006), even those PNH patients within our group, which supports the idea that the CC is involved in brain networks.

Thus, our results, in conjunction with previous reports, suggest extensive DTI changes in the CC of patients with PNH. Notably, our results and the majority of other reports find a similar pattern of DTI changes: a reduction in FA in association with elevated MD. The reductions in anisotropy may result from disruptions in axons or myelin (Pierpaoli et al., 2001). Elevated MD may relate to decreased synaptic density or abnormal cellular composition (Song et al., 2002).

Previous research has indicated that abnormal corpus callosum morphology is a common feature of PNH, with the greatest volume reduction in the splenium (Pardoe et al., 2015). This is in accordance with our diffusion findings showed that both FA and MD of splenium segment were significantly changed compared to HCs. The parameters of “volume” and “DTI metrics” are based on different modalities and there is correlation between them. Volume is an indicator of morphology, whereas DTI metrics particular measure anisotropy (FA) and diffusivity (MD). Additionally, except for the FA levels in the splenium, we found no correlation between DTI metrics of the CC segments and disease duration in PNH patients, indicating that the structural alteration was stable and independent of disease duration. Meanwhile, the relationship between FA in the splenium and epilepsy duration suggests that ongoing seizures may cause diffusion changes rather than these DTI changes existing prior to seizure onset.

Heterozygous loss of function mutations within the *Filamin A* gene located in Xq28 are the most frequent cause of bilateral symmetric PNH. These mutations are found predominantly in females, and cause various phenotypes. The gene product of *FLNA* is a large cytoplasmic actin-binding and cross-linking protein with diverse functions (Sheen, 2014), including initiation of cell migration, blood coagulation, and maintenance of blood vessel wall integrity (Baldassarre et al., 2009). Functional imaging indicates that the *FLNA* mutation-associated ectopic cortical neurons are functionally integrated into motor circuits (Lange et al., 2004). Abnormal functional connectivity arising from *FLNA* mutations might influence the structure or activity of brain areas when *FLNA* is expressed.

In the *FLNA*-mutated PNH subgroup, patients showed significantly decreased FA in all segments, and increased MD in the genu and splenium, as compared to HCs and *FLNA*-nonmutated patients. However, it is important to note that all the eleven *FLNA*-mutated patients had bilateral PNH lesions, whereas some of the *FLNA*-nonmutated patients had unilateral PNH lesions. It is possible that the differences in diffusion are simply associated with differences in heterotopia burden. Therefore, further ANCOVA analysis was performed and the complementary findings accord with our original results completely, suggesting FA or MD difference in the CC between *FLNA*-mutated and *FLNA*-nonmutated groups was not affected by PNH burden. Additionally, due to the small sample size, the test power was relatively low. It is also important to note that these findings might be impacted by our patients' long-standing use of AEDs. *FLNA* is always considered to be essential for neuronal migration in humans (Carabalona et al., 2012). A previous study indicates that *Filamin A* interacting protein (FILIP) plays a role in the proper positioning of callosal projection neurons (Yagi et al., 2016), which may link callosal projections to the pathogenesis of brain disorders. Overall, the difference with respect to *FLNA* mutation suggested a special role of *FLNA* on CC integrity in this disorder, might also indicate that *FLNA*-mutated and nonmutated PNH patients had distinct pathological mechanisms.

Several limitations should be addressed. First, AEDs may have an effect on white matter integrity as none of the patients were drug naïve. Then, a limited number of participants were recruited in the current study (especially in *FLNA*-mutated patient groups), which decreased the statistical power of our analysis. Therefore, our data should be considered as indicative of an effect of *FLNA* mutation on CC segments' DTI metrics. Additionally, the lack of cognitive and psychological assessment limited our ability to correlate brain connectivity to neurobehavioral performance. Finally, our study had a cross-sectional design. It was difficult to determine the causal relationship between CC diffusion alterations and age in PNH patients, though a linear relationship was observed. A longitudinal design should be used, in future studies, to address this issue.

Acknowledgement

We would like to thank all the patients with PNH and healthy controls who took part in this study and provided their information.

Funding

This study was supported by the National 863 project (Grant No. 2015AA020505) and National Natural Science Foundation of China (Grant No. 81420108014, 81371529 and 81401079).

Conflict of interest

None.

References

Andrade, C.S., Leite, C.C., Otaduy, M.C., Lyra, K.P., Valente, K.D., Yasuda, C.L., Beltramini, G.C., Beaulieu, C., Gross, D.W., 2014. Diffusion abnormalities of the corpus callosum in patients with malformations of cortical development and epilepsy. Epilepsy Res. 108, 1533–1542.

Baldassarre, M., Razinia, Z., Burande, C.F., Lamsoul, I., Lutz, P.G., Calderwood, D.A., 2009. Filamins regulate cell spreading and initiation of cell migration. PLoS One 4, e7830.

Battaglia, G., Chiapparini, L., Franceschetti, S., Freri, E., Tassi, L., Bassanini, S., Villani, F., Spreafico, R., D'Incerti, L., Granata, T., 2006. Periventricular nodular heterotopia: classification, epileptic history, and genesis of epileptic discharges. Epilepsia 47, 86–97.

Caligiuri, M.E., Labate, A., Cherubini, A., Mumoli, L., Ferlazzo, E., Aguglia, U., Quattrone, A., Gambardella, A., 2016. Integrity of the corpus callosum in patients with benign temporal lobe epilepsy. Epilepsia 57, 590–596.

Carabalona, A., Beguin, S., Pallesi-Pocachard, E., Buhler, E., Pellegrino, C., Arnaud, K., Hubert, P., Oualha, M., Siffroi, J.P., Khantane, S., Coupry, I., Goizet, C., Gelot, A.B., Represa, A., Cardoso, C., 2012. A glial origin for periventricular nodular heterotopia caused by impaired expression of Filamin-A. Hum. Mol. Genet. 21, 1004–1017.

Chang, B.S., Katzir, T., Liu, T., Corriveau, K., Barzillai, M., Apse, K.A., Bodell, A., Hackney, D., Alsop, D., Wong, S.T., Walsh, C.A., 2007. A structural basis for reading fluency: white matter defects in a genetic brain malformation. Neurology 69, 2146–2154.

Christodoulou, J.A., Walker, L.M., Del Tufo, S.N., Katzir, T., Gabrieli, J.D., Whitfield-Gabrieli, S., Chang, B.S., 2012. Abnormal structural and functional brain connectivity in gray matter heterotopia. Epilepsia 53, 1024–1032.

Concha, L., Gross, D.W., Wheatley, B.M., Beaulieu, C., 2006. Diffusion tensor imaging of time-dependent axonal and myelin degradation after corpus callosotomy in epilepsy patients. NeuroImage 32, 1090–1099.

Concha, L., Beaulieu, C., Wheatley, B.M., Gross, D.W., 2007. Bilateral white matter diffusion changes persist after epilepsy surgery. Epilepsia 48, 931–940.

Eriksson, S.H., Rugg-Gunn, F.J., Symms, M.R., Barker, G.J., Duncan, J.S., 2001. Diffusion tensor imaging in patients with epilepsy and malformations of cortical development. Brain 124, 617–626.

Filippi, C.G., Maxwell, A.W., Watts, R., 2013. Magnetic resonance diffusion tensor imaging metrics in perilesional white matter among children with periventricular nodular gray matter heterotopia. Pediatr. Radiol. 43, 1196–1203.

Guerrini, R., Dobyns, W.B., 2014. Malformations of cortical development: clinical features and genetic causes. Lancet Neurol. 13, 710–726.

Hofer, S., Frahm, J., 2006. Topography of the human corpus callosum revisited—comprehensive fiber tractography using diffusion tensor magnetic resonance imaging. NeuroImage 32, 989–994.

Huang, H., Zhang, J., Jiang, H., Wakana, S., Poetscher, L., Miller, M.I., van Zijl, P.C., Hillis, A.E., Wytik, R., Mori, S., 2005. DTI tractography based parcellation of white matter: application to the mid-sagittal morphology of corpus callosum. NeuroImage 26, 195–205.

Ji, G.J., Zhang, Z., Xu, Q., Zang, Y.F., Liao, W., Lu, G., 2014. Generalized tonic-clonic seizures: aberrant interhemispheric functional and anatomical connectivity. Radiology 271, 839–847.

Kini, L.G., Gee, J.C., Litt, B., 2016. Computational analysis in epilepsy neuroimaging: a survey of features and methods. Neuroimage Clin. 11, 515–529.

Lange, M., Winner, B., Muller, J.L., Marienhagen, J., Schroder, M., Aigner, L., Uyanik, G., Winkler, J., 2004. Functional imaging in PNH caused by a new FilaminA mutation. Neurology 62, 151–152.

Lange, M., Kasper, B., Bohring, A., Rutsch, F., Kluger, G., Hoffjan, S., Spranger, S., Behnecke, A., Ferbert, A., Hahn, A., Oehl-Jaschkowitz, B., Graul-Neumann, L., Diepold, K., Schreyer, I., Bernhard, M.K., Mueller, F., Siebers-Renelt, U., Beleza-Meireles, A., Uyanik, G., Janssens, S., Boltshauser, E., Winkler, J., Schuierer, G., Hehr, U., 2015. 47 patients with FLNA associated periventricular nodular heterotopia. Orphanet J. Rare Dis. 10, 134.

Leventer, R.J., Phelan, E.M., Coleman, L.T., Kean, M.J., Jackson, G.D., Harvey, A.S., 1999. Clinical and imaging features of cortical malformations in childhood. Neurology 53, 715–722.

Liao, W., Zhang, Z., Pan, Z., Mantini, D., Ding, J., Duan, X., Luo, C., Wang, Z., Tan, Q., Lu, G., Chen, H., 2011. Default mode network abnormalities in mesial temporal lobe epilepsy: a study combining fMRI and DTI. Hum. Brain Mapp. 32, 883–895.

Liu, M., Concha, L., Beaulieu, C., Gross, D.W., 2011. Distinct white matter abnormalities in different idiopathic generalized epilepsy syndromes. Epilepsia 52, 2267–2275.

Liu, W., Yan, B., An, D., Xiao, J., Hu, F., Zhou, D., 2017. Sporadic periventricular nodular heterotopia: classification, phenotype and correlation with Filamin A mutations. Epilepsy Res. 133, 33–40.

Long, Z., Xu, Q., Miao, H.H., Yu, Y., Ding, M.P., Chen, H., Liu, Z.R., Liao, W., 2017. Thalamocortical dysconnectivity in paroxysmal kinesigenic dyskinesia: combining functional magnetic resonance imaging and diffusion tensor imaging. Mov. Disord. 32, 592–600.

Pardoe, H.R., Mandelstam, S.A., Hiess, R.K., Kuzniecky, R.I., Jackson, G.D., 2015. Quantitative assessment of corpus callosum morphology in periventricular nodular heterotopia. Epilepsy Res. 109, 40–47.

Parrini, E., Ramazzotti, A., Dobyns, W.B., Mei, D., Moro, F., Veggiotti, P., Marini, C., Brilstra, E.H., Dalla Bernardina, B., Goodwin, L., Bodell, A., Jones, M.C., Nangeroni, M., Palmeri, S., Said, E., Sander, J.W., Striano, P., Takahashi, Y., Van Maldergem, L., Leonardi, G., Wright, M., Walsh, C.A., Guerrini, R., 2006. Periventricular heterotopia: phenotypic heterogeneity and correlation with Filamin A mutations. Brain 129, 1892–1906.

Parrini, E., Mei, D., Pisanti, M.A., Catarzi, S., Pucatti, D., Bianchini, C., Mascalchi, M., Bertini, E., Morrone, A., Cavaliere, M.L., Guerrini, R., 2015. Familial periventricular nodular heterotopia, epilepsy and Melnick-Needles Syndrome caused by a single FLNA mutation with combined gain-of-function and loss-of-function effects. J. Med. Genet. 52, 405–412.

Pierpaoli, C., Barnett, A., Pajevic, S., Chen, R., Penix, L.R., Virta, A., Basser, P., 2001. Water diffusion changes in Wallerian degeneration and their dependence on white matter architecture. NeuroImage 13, 1174–1185.

Pisano, T., Barkovich, A.J., Leventer, R.J., Squier, W., Scheffer, I.E., Parrini, E., Blaser, S., Marini, C., Robertson, S., Tortorella, G., Rosenow, F., Thomas, P., McGillivray, G., Andermann, E., Andermann, F., Berkovic, S.F., Dobyns, W.B., Guerrini, R., 2012. Peritrigonal and temporo-occipital heterotopia with corpus callosum and cerebellar dysgenesis. Neurology 79, 1244–1251.

Shafi, M.M., Vernet, M., Klooster, D., Chu, C.J., Boric, K., Barnard, M.E., Romatoski, K., Westover, M.B., Christodoulou, J.A., Gabrieli, J.D., Whitfield-Gabrieli, S., Pascual-Leone, A., Chang, B.S., 2015. Physiological consequences of abnormal connectivity in a developmental epilepsy. Ann. Neurol. 77, 487–503.

Sheen, V.L., 2014. Filamin A mediated Big2 dependent endocytosis: from apical abscission to periventricular heterotopia. Tissue Barriers 2, e29431.

Sheen, V.L., Dixon, P.H., Fox, J.W., Hong, S.E., Kinton, L., Sisodiya, S.M., Duncan, J.S., Dubeau, F., Scheffer, I.E., Schachter, S.C., Wilner, A., Henchy, R., Crino, P., Kamuro, K., DiMario, F., Berg, M., Kuzniecky, R., Cole, A.J., Bromfield, E., Biber, M., Schomer, D., Wheless, J., Silver, K., Mochida, G.H., Berkovic, S.F., Andermann, F., Andermann, E., Dobyns, W.B., Wood, N.W., Walsh, C.A., 2001. Mutations in the X-linked filamin 1 gene cause periventricular nodular heterotopia in males as well as in females. Hum. Mol. Genet. 10, 1775–1783.

Song, S.K., Sun, S.W., Ramsbottom, M.J., Chang, C., Russell, J., Cross, A.H., 2002. Dysmyelination revealed through MRI as increased radial (but unchanged axial) diffusion of water. NeuroImage 17, 1429–1436.

Thivard, L., Lehericy, S., Krainik, A., Adam, C., Dormont, D., Chiras, J., Baulac, M., Dupont, S., 2005. Diffusion tensor imaging in medial temporal lobe epilepsy with hippocampal sclerosis. NeuroImage 28, 682–690.

Witelson, S.F., 1989. Hand and sex differences in the isthmus and genu of the human corpus callosum. A postmortem morphological study. Brain 112 (Pt 3), 799–835.

Yagi, H., Oka, Y., Komada, M., Xie, M.J., Noguchi, K., Sato, M., 2016. Filamin A interacting protein plays a role in proper positioning of callosal projection neurons in the cortex. Neurosci. Lett. 612, 18–24.